

# Bacteria meets influenza A virus: A bioluminescence mouse model of *Escherichia coli* O157:H7 following influenza A virus/Puerto Rico/ 8/34 (H1N1) strain infection

Zhongyi Wang<sup>1,\*</sup>, Hang Chi<sup>1,\*</sup>, Xiwen Wang<sup>1</sup>,  
Wenliang Li<sup>1,2,3</sup>, Zhiping Li<sup>1</sup>, Jiaming Li<sup>1</sup>,  
Yingying Fu<sup>1</sup>, Bing Lu<sup>1</sup>, Zhiping Xia<sup>1</sup>, Jun Qian<sup>1</sup>  
and Linna Liu<sup>1</sup>

## Abstract

**Objective:** To develop a bioluminescence-labelled bacterial infection model to monitor the colonization and clearance process of *Escherichia coli* O157:H7 in the lungs of mice following influenza A virus/Puerto Rico/8/34 (H1N1) strain (IAV/PR8) infection.

**Methods:** BALB/c mice were administered IAV/PR8 or 0.01 M phosphate-buffered saline (PBS; pH 7.4) intranasally 4 days prior to intranasal administration of  $1 \times 10^7$  colony-forming units (CFU) of *E. coli* O157:H7-lux. Whole-body bioluminescent signals were monitored at 10 min, 4 h, 8 h, 12 h, 16 h and 24 h post-bacterial infection. Lung bioluminescent signals and bacterial load (CFU/g) were monitored at 4 h, 8 h, 12 h, 16 h and 24 h post-bacterial infection.

**Results:** Prior IAV/PR8 infection of mice resulted in a higher level of bacterial colonization and a lower rate of bacterial clearance from the lungs compared with mice treated with PBS. There were also consistent findings between the bioluminescence imaging and the CFU measurements in terms of identifying bacterial colonization and monitoring the clearance dynamics of *E. coli* O157:H7-lux in mouse lungs.

<sup>1</sup>Academy of Military Medical Sciences, Beijing, China

<sup>2</sup>Jilin Medical University, Jilin, Jilin Province, China

<sup>3</sup>Key Laboratory of Preparation and Application of Environmentally Friendly Materials, Ministry of Education, Jilin Normal University, Changchun, Jilin Province, China

\*These authors contributed equally to this work.

## Corresponding authors:

Zhiping Xia, Jun Qian and Linna Liu, Academy of Military Medical Sciences, 27 Taiping Road, Beijing 100850, China. Emails: ammszpxia@163.com; qianj1970@126.com; liulinna7@126.com



**Conclusion:** This novel bioluminescence-labelled bacterial infection model rapidly detected bacterial colonization of the lungs and monitored the clearance dynamics of *E. coli* O157:H7-lux following IAV/PR8 infection.

### Keywords

Bioluminescence imaging, *Escherichia coli* O157:H7, co-infection, influenza A virus

Date received: 15 March 2018; accepted: 26 April 2018

### Introduction

Spanish flu (in 1918), Asian flu (in 1957), Hong Kong flu (in 1968) and swine flu (in 2009) are examples of previous influenza pandemics that had a profound impact on human health and social stability. Approximately 400 000 deaths worldwide are caused by influenza viruses every year.<sup>1</sup> Bacterial co-infection following influenza virus infection might be one of the main reasons for severe disease and mortality during influenza episodes.<sup>2,3</sup> Research has mainly focused on the pathogenicity of the influenza virus and mechanisms of bacterial co-infections following viral infection.<sup>4</sup> A mouse model to visualize and monitor whole body colonization and the progress of clearance of bacteria in the lungs following influenza virus infection, which could be very useful for research into drug evaluation and clinical diagnosis, has not been reported previously in the published literature.

Traditional methods, such as quantitative polymerase chain reaction and counting of colony-forming units (CFU), need high numbers of experimental animals and a plentiful supply of research materials to discover the whole process of bacterial colonization and clearance in the lungs.<sup>5</sup> The results from these traditional methods do not completely represent the reality of bacterial colonization and clearance *in vivo*.

Hence, establishing a mouse model to visualize and monitor the dynamics of colonization and clearance might be a novel approach to track bacterial colonization and clearance *in vivo* following influenza A virus (IAV) infection.

In a previous study, the current authors found that *Escherichia coli* O157 could reproduce in the lungs of mice after an intraperitoneal injection, which suggested that this bacterium might be used as a tool to explore the mechanisms of bacterial infection following IAV infection.<sup>6</sup> In addition, the bacterial luciferase gene cassette (luxCDABE) is an ideal bioreporter for real-time monitoring of the dynamics of bacterial colonization and clearance because it is a fully autonomous, substrate-free bioluminescent reporter system available in a prokaryotic or eukaryotic host background. pBBR-lux is a broad host range plasmid vector that carries the luxCDABE operon for the construction of bioluminescent Gram-negative bacteria.<sup>7</sup> Compared with a chromosome-based reporter, the plasmid-based lux reporter could offer high-resolution and high-definition imaging of the pathophysiological processes of infection because it can be maintained at higher copies, which can increase the sensitivity of bioluminescent signals.<sup>8</sup>

In this current study, a well-developed strain of Gram-negative bacteria, *E. coli*

O157:H7-lux, expressing bacterial luciferase was used to perform intranasal infection in mice 4 days post-influenza A virus/Puerto Rico/8 (IAV/PR8) infection. Using bioluminescence imaging, the colonization and clearance process of *E. coli* O157:H7-lux in the lung following IAV/PR8 infection was monitored in this mouse model.

## Materials and methods

### Mice

Six-week-old female BALB/c mice (weight range 20–22 g) were purchased from the Experimental Animal Centre, Liaoning, China and were housed in specific pathogen-free conditions at the Experimental Animal Centre. Ten animals were used for each group. The animals were housed using a 12-h light/12-h dark cycle with free access to food and water. All animal studies were conducted in strict accordance with the guidelines for animal welfare of the World Organization for Animal Health. Experimental protocols involving animals were approved by the Animal Care and Use Committee of Academy of Military Medical Sciences, Beijing, China (approval number: SCXK 2016-0008).

### Influenza virus and the viral infection method

The influenza virus A/Puerto Rico/8/34 (H1N1) strain was used for viral infection *in vivo*. The IAV/PR8 source and culture conditions were as described in a previous study.<sup>9</sup> Under anaesthesia, mice were intranasally infected with 50  $\mu$ l of 0.01 M phosphate-buffered saline (PBS; pH 7.4) containing 50 EID<sub>50</sub> of IAV/PR8 or 0.01 M PBS (pH 7.4) alone as a control.

### Construction of bioluminescent strains

Bioluminescent bacteria, *E. coli* O157:H7-lux, were constructed by the introduction of the pBBR-lux plasmid as described previously.<sup>10</sup> The recombinant plasmid pBBR-lux and the monitoring of the bioluminescent intensity and stability have been described previously.<sup>6,7</sup> The luciferase-expressing bioluminescent strains were detected using a NightOWL II LB 983 *in vivo* Imaging System (Berthold Technologies, Bad Wildbad, Germany).

*Escherichia coli* O157:H7, which was used to infect the mice in this study, has been investigated in a previous study as a plasmid-based bioluminescent Gram-negative bacterial strain.<sup>6</sup> The pBBR-lux plasmid was introduced into *E. coli* O157:H7 and was successfully verified using a NightOWL II LB983 *in vivo* Imaging System.<sup>6</sup> There was a significant correlation between bioluminescent signals of this bioluminescent strain.<sup>6</sup> Similar growth kinetics were found between *E. coli* O157:H7 and its parent strain.<sup>6</sup> The plasmid in *E. coli* O157:H7 exhibited high stability, which was determined by the ratio between bioluminescence normalized for CFU under nonselective conditions versus kanamycin-selected conditions.<sup>6</sup>

In addition, in a previous study, mice were injected intraperitoneally with *E. coli* O157:H7 and this strain reproduced in most organs of the body.<sup>6</sup> The previous study also showed the overall counts per second (CPS) and the bacterial loads of five different organs (gastrointestinal tract, liver, spleen, kidney and lung).<sup>6</sup> These results demonstrated that *E. coli* O157:H7 presented a risk of infection in mammalian lungs so it was an appropriate model to use to study bacterial co-infections following IAV infection.<sup>6</sup>

These bioluminescent stains were grown in tryptic soy broth (TSB) with shaking or on TSB agar plates at 37°C.

Kanamycin (50 µg/ml; Sigma-Aldrich, Shanghai, China) was added to the medium as required.

### Bacterial infection and in vivo imaging

All mice that had been infected with either IAV/PR8 or 0.01 M PBS (pH 7.4) were subsequently intranasally infected with  $1 \times 10^7$  CFU of *E. coli* O157:H7-lux. The amount of time between IAV/PR8 infection and the subsequent bacterial infection was 4 days. The imaging time points were 10 min, 4 h, 8 h, 12 h, 16 h and 24 h post-bacterial infection. Animals were anaesthetized with 3% isoflurane and then scanned using a NightOWL II LB 983 *in vivo* Imaging System. The calculation of overall CPS was performed for both the whole body and the lungs. The CFU assay method was briefly described in a previous study and was calculated for the lungs.<sup>10</sup>

### Results

Using bioluminescent whole-body imaging *in vivo*, the bioluminescent signal produced by *E. coli* O157:H7-lux could be detected in both groups infected by IAV/PR8 or PBS control (Figure 1). From 10 min to 24 h, the signal intensity in the group infected with IAV/PR8 was higher than the group infected with PBS control. The signal intensity of the PBS group reached a peak at 8 h. However, the signal intensity of the IAV/PR8 group increased until 12 h.

Figure 2 shows the bioluminescence imaging of the lungs in mice. The difference in the bioluminescence intensity in the lungs between the two groups was similar to the results obtained for the whole-body imaging, but the CPS in the lungs was higher than that for the whole-body imaging. The bioluminescence signal intensity of the IAV/PR8 group was more diffuse in the

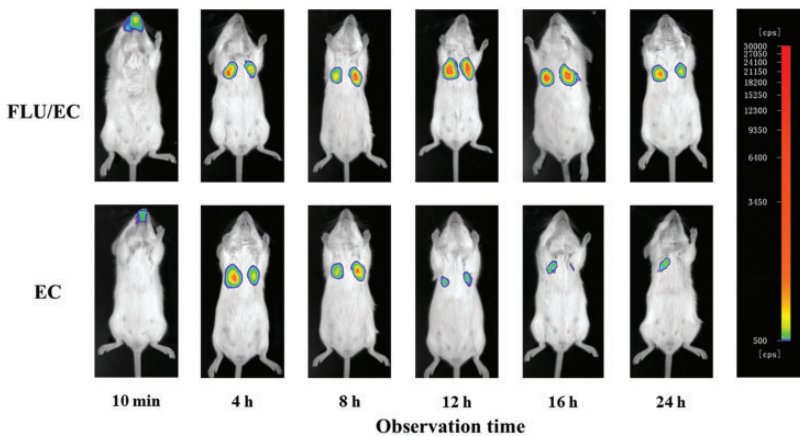


**Figure 1.** Bioluminescence imaging in two representative BALB/c mice that were injected intranasally with the influenza A/Puerto Rico/8/34 (H1N1) strain or 0.01 M phosphate-buffered saline (PBS; pH 7.4) 4 days prior to intranasal infection with  $1 \times 10^7$  colony-forming units of *Escherichia coli* O157:H7-lux. Mice were imaged at 10 min, 4 h, 8 h, 12 h, 16 h and 24 h post-bacterial infection using a NightOWL II LB 983 *in vivo* Imaging System. The colour bar on the right shows the intensity of the bioluminescence signal coded in the picture from indigo (500 counts per second [CPS]) to red (30 000 CPS). FLU/EC, influenza A/Puerto Rico/8/34 (H1N1) strain and *E. coli* O157:H7; EC, *E. coli* O157:H7 only. The colour version of this figure is available at: <http://imr.sagepub.com>.

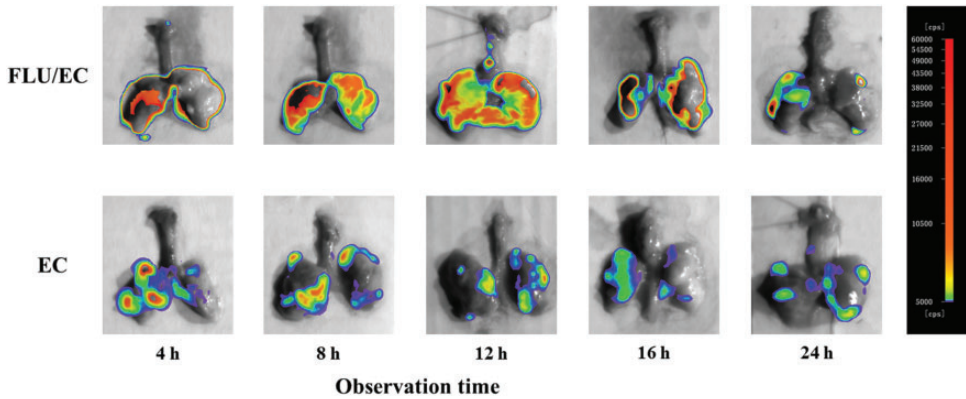


**Figure 2.** Bioluminescence imaging of the lungs of two representative BALB/c mice that were injected intranasally with the influenza A/Puerto Rico/8/34 (H1N1) strain or 0.01 M phosphate-buffered saline (PBS; pH 7.4) 4 days prior to intranasal infection with  $1 \times 10^7$  colony-forming units of *Escherichia coli* O157:H7-lux. Mice were imaged at 4 h, 8 h, 12 h, 16 h and 24 h post-bacterial infection using a NightOWL II LB 983 *in vivo* Imaging System. The colour bar on the right shows the intensity of the bioluminescence signal coded in the picture from indigo (500 counts per second [CPS]) to red (60 000 CPS). FLU/EC, influenza A/Puerto Rico/8/34 (H1N1) strain and *E. coli* O157:H7; EC, *E. coli* O157:H7 only. The colour version of this figure is available at: <http://imr.sagepub.com>.

lung at 8 h and 12 h, while the distribution of the bioluminescence signal in the PBS group was more concentrated.

A CFU experiment was performed to calculate the bacterial loads in the lungs so that this could be compared with the CPS values. The mean  $\pm$  SD CPS values for whole-body imaging for the two groups are shown in Figure 3a. The mean  $\pm$  SD CPS values and the mean  $\pm$  SD CFU/g for the lungs of the two groups are shown in Figure 3b. These results demonstrated that the bacterial loads and the CPS values were similar within each group in the lungs at each time point and showed similar changes over time.

## Discussion

Previous research has shown that the immune system in a typical mouse lung will be activated when pathogens colonize the respiratory tract and the inflammatory

response can clear up to  $10^5$  bacteria within 4–12 h.<sup>11</sup> In this current study, the bioluminescence mouse model showed that the overall pattern of bacterial reproduction followed an ‘increase-then-decrease’, which suggests that the immune system provided a clearance function in response to the colonization of the body and lungs by bacteria. There was an obvious clearance of bacteria in mice after 8 h in the PBS group based on the whole-body and lung bioluminescence imaging. However, this clearance function was much weaker in the IAV/PR8 group, which resulted in continued reproduction of the bacteria in the mice. These results suggest that the clearance function of the immune system might be adversely affected by IAV/PR8 infection. While type I interferons play an important role in anti-viral responses, the cell factors involved in interferon signalling could also disrupt anti-bacterial responses.<sup>12</sup> Although researchers have found some evidence for an

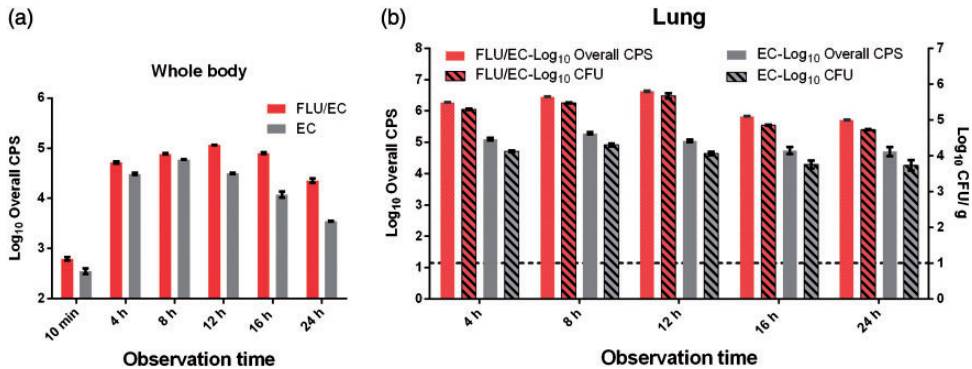


**Figure 3.** Results of the bioluminescence imaging of whole bodies and lungs and the bacterial loads in the lungs of BALB/c mice that were injected intranasally with the influenza A/Puerto Rico/8/34 (H1N1) strain or 0.01 M phosphate-buffered saline (PBS; pH 7.4) 4 days prior to infection with  $1 \times 10^7$  colony-forming units of *Escherichia coli* O157:H7-lux. The whole bodies were imaged at 10 min, 4 h, 8 h, 12 h, 16 h and 24 h post-bacterial infection (a) and the lungs at 4 h, 8 h, 12 h, 16 h and 24 h post-bacterial infection (b) using a NightOWL II LB 983 *in vivo* Imaging System. (a) Counts per minute (CPS) for the whole-body bioluminescence imaging results expressed as mean  $\pm$  SD of three independent experiments. (b) Bacterial load in colony-forming units (CFU)/g of lung and overall CPS of the lungs with the results expressed as mean  $\pm$  SD of three independent experiments. The horizontal dotted line indicates the detection limit of the bacterial load (10 CFU). FLU/EC, influenza A/Puerto Rico/8/34 (H1N1) strain and *E. coli* O157:H7; EC, *E. coli* O157:H7 only. The colour version of this figure is available at: <http://imr.sagepub.com>.

explanation as to why the immune system might be disrupted by viral infection, such as suppression of phagocytic activity and dysfunction of macrophages and neutrophils through reduced granulocyte-colony stimulating factor production,<sup>9,12,13</sup> the increased risk of secondary bacterial infection in the lung following IAV infection needs further research into the changes in the immune response, pathogenesis and drug therapy. In these areas of research, bioluminescence imaging technology might offer unique advantages in terms of providing rapid visual monitoring of bacterial colonization and clearance dynamics.

In the current study, there was a difference between the patterns of bioluminescent signal distribution in the lungs between the IAV/PR8 and PBS groups. Although the bioluminescent signals might not completely represent the actual site of bacterial colonization, these results might reflect the general conditions of bacterial distribution

in the lungs. The bioluminescence signal intensity of the IAV/PR8 group was more diffuse in the lungs at 8 h and 12 h, while the distribution of the bioluminescence signal in the PBS group was more concentrated. This between-group difference in the distribution of bacteria in the lungs might be associated with a difference in the susceptibility to bacterial colonization following IAV infection.<sup>14</sup> Influenza virus reproduction in epithelial cells of the lungs can lead to tissue damage, which might then result in more sites being suitable for bacterial colonization in the tracheobronchial tree.<sup>15,16</sup> For example, in lungs that have been exposed to IAV preceding the bacterial infection, inaccessible receptors in the lower respiratory tract might become available to invading bacteria.<sup>17</sup> This increased binding to receptors, such as cryptic receptors,<sup>18</sup> could help the invading bacteria rapidly reproduce and spread all over the lung. This in turn might further aggravate the

burden on the immune system in the lungs, leading to persistent bacterial growth. These reasons might explain why there was a difference in the bacterial distribution in the lungs between the two groups in the current study.

The current study also demonstrated consistent findings between the bioluminescence imaging and the CFU measurements in terms of identifying bacterial colonization and monitoring the clearance dynamics of *E. coli* O157:H7-lux in the lungs of mice. These findings suggest that this novel bioluminescence-labelled bacterial infection model might be used as an efficient and rapid tool for future studies in pulmonary infections and drug screening.

In conclusion, this novel bioluminescence-labelled bacterial infection model was successfully used to rapidly detect bacterial colonization of the lungs and to monitor the clearance dynamics of *E. coli* O157:H7-lux in the lungs of mice following IAV/PR8 infection. The results suggested that following IAV/PR8 infection, there was reduced bacterial clearance by the immune system and increased susceptibility to bacteria in the lungs of mice. In the future, bacterial co-infections following IAV infection could be further explored using different types of bioluminescence-labelled bacteria and more novel imaging techniques,<sup>19,20</sup> which might help with the timely and efficient development of novel anti-bacterial treatment strategies.

### Declaration of conflicting interests

The authors declare that there are no conflicts of interest.

### Funding

Financial support for this study came from the National Major Research & Development Programme (no. 2016YFD0500505), from the National Natural Science Foundation of China (no. 31402221), from the Grant of Jilin Province

Science & Technology Committee (no. 20170520149JH), the Department of Education of Jilin Province (no. JJKH20170408KJ), the Youth Foundation Project of Jilin Province Health and Family Planning Commission (no. 2016Q053), from the Jilin City Science & Technology Innovation and Development Projects (no. 20166032) and the Open Project Programme of the Key Laboratory of Preparation and Application of Environmentally Friendly Materials (Jilin Normal University), Ministry of Education, China (no. 2017006). The funders had no role in the study design, data collection and analysis, decision to publish or preparation of the manuscript.

### References

1. King JC, Schweinle JE, Hatchett RJ, et al. Surges of advanced medical support associated with influenza outbreaks. *Epidemiol Infect* 2017; 145: 2409–2416. DOI: 10.1017/S095026881700111X.
2. Guarner J, Paddock CD, Shieh WJ, et al. Histopathologic and immunohistochemical features of fatal influenza virus infection in children during the 2003–2004 season. *Clin Infect Dis* 2006; 43: 132–140. DOI: 10.1086/505122.
3. McDanel JS, Perencevich EN, Storm J, et al. Increased Mortality Rates Associated with Staphylococcus aureus and Influenza Co-infection, Maryland and Iowa, USA (1). *Emerg Infect Dis* 2016; 22: 1253–1256. DOI: 10.3201/eid2207.151319.
4. Jia L, Xie J, Zhao J, et al. Mechanisms of severe mortality-associated bacterial co-infections following influenza virus infection. *Front Cell Infect Microbiol* 2017; 7: 338. DOI: 10.3389/fcimb.2017.00338.
5. Bakaletz LO. Developing animal models for polymicrobial diseases. *Nat Rev Microbiol* 2004; 2: 552–568. DOI: 10.1038/nrmicro928.
6. Wang X, Chi H, Li Q, et al. Influence of Antibiotic Pressure on Five Plasmid-based Bioluminescent Gram-negative Bacterial Strains. *Mol Imaging Biol* 2018; 20: 21–26. DOI: 10.1007/s11307-017-1110-x.
7. Wang X, Li Z, Li B, et al. Bioluminescence imaging of colonization and clearance

- dynamics of Brucella Suis Vaccine Strain S2 in mice and guinea pigs. *Mol Imaging Biol* 2016; 18: 519–526. DOI: 10.1007/s11307-015-0925-6.
8. Sun Y, Connor MG, Pennington JM, et al. Development of bioluminescent bioreporters for in vitro and in vivo tracking of *Yersinia pestis*. *PLoS One* 2012; 7: e47123. DOI: 10.1371/journal.pone.0047123.
  9. Ishikawa H, Fukui T, Ino S, et al. Influenza virus infection causes neutrophil dysfunction through reduced G-CSF production and an increased risk of secondary bacteria infection in the lung. *Virology* 2016; 499: 23–29. DOI: 10.1016/j.virol.2016.08.025.
  10. Wang X, Li Z, Dong X, et al. Development of bioluminescent *Cronobacter sakazakii* ATCC 29544 in a mouse model. *J Food Prot* 2015; 78: 1007–1012. DOI: 10.4315/0362-028X.JFP-14-482.
  11. Sun K and Metzger DW. Inhibition of pulmonary antibacterial defense by interferon-gamma during recovery from influenza infection. *Nat Med* 2008; 14: 558–564. DOI: 10.1038/nm1765.
  12. Lee B, Robinson KM, McHugh KJ, et al. Influenza-induced type I interferon enhances susceptibility to gram-negative and gram-positive bacterial pneumonia in mice. *Am J Physiol Lung Cell Mol Physiol* 2015; 309: L158–L167. DOI: 10.1152/ajplung.00338.2014.
  13. Shahangian A, Chow EK, Tian X, et al. Type I IFNs mediate development of post-influenza bacterial pneumonia in mice. *J Clin Invest* 2009; 119: 1910–1920. DOI: 10.1172/JCI35412.
  14. Childs RA, Palma AS, Wharton S, et al. Receptor-binding specificity of pandemic influenza A (H1N1) 2009 virus determined by carbohydrate microarray. *Nat Biotechnol* 2009; 27: 797–799. DOI: 10.1038/nbt0909-797.
  15. Metzger DW and Sun K. Immune dysfunction and bacterial coinfections following influenza. *J Immunol* 2013; 191: 2047–2052. DOI: 10.4049/jimmunol.1301152.
  16. Peteranderl C, Sznajder JI, Herold S, et al. Inflammatory responses regulating alveolar ion transport during pulmonary infections. *Front Immunol* 2017; 8: 446. DOI: 10.3389/fimmu.2017.00446
  17. McCullers JA and Bartmess KC. Role of neuraminidase in lethal synergism between influenza virus and *Streptococcus pneumoniae*. *J Infect Dis* 2003; 187: 1000–1009. DOI: 10.1086/368163.
  18. McCullers JA and Tuomanen EI. Molecular pathogenesis of pneumococcal pneumonia. *Front Biosci* 2001; 6: D877–D889.
  19. An FF, Chan M, Kommidi H, et al. Dual PET and near-infrared fluorescence imaging probes as tools for imaging in oncology. *AJR Am J Roentgenol* 2016; 207: 266–273. 2016/05/26. DOI: 10.2214/ajr.16.16181.
  20. An FF and Zhang XH. Strategies for preparing albumin-based nanoparticles for multifunctional bioimaging and drug delivery. *Theranostics* 2017; 7: 3667–3689. 2017/11/08. DOI: 10.7150/thno.19365.